kcal/mol at 1000 bar, as calculated by eq 12 with $f = 0.09$ at 25 °C. If we give some credence in a more qualitative sense to the estimates of the "isolated-chain" values of the quantities E_0, V, and U,[11] it appears that our values are, as expected, much larger.

These calculations show that with both models we obtain reasonable results for quantities like hole volumes and hole formation energies or isomerization energy barriers. This is not unexpected since the physical basis of both models is simple and not too different. The isomerization model gives to the hole model a more precise interpretation which, however, cannot be validated or invalidated by this kind of measurement.

Acknowledgment. We gratefully acknowledge the generous financial support of the "Minister für Wissenschaft und Forschung of NRW", the DFG, and the Fonds der Chemischen Industrie.

References and Notes

(1) McCrum, N. G.; Read, B. E.; Williams, G., Eds. "Anelastic and Dielectric Effects in Polymeric Solids"; Wiley: New York, 1967.
(2) Karasz, F. G., Ed. "Dielectric Properties of Polymers"; Plenum Press: New York, 1972.
(3) Hedvig, P. "Dielectric Spectroscopy of Polymers"; Adam Hilger Ltd.: Bristol, 1977.
(4) Lindsey, C. P.; Patterson, G. D.; Stevens, J. R. *J. Polym. Sci., Polym. Phys. Ed.* **1979**, *17*, 1547.
(5) Lee, H.; Jamieson, A. M.; Simha, R. *J. Macromol. Sci., Phys.* **1980**, *B18*, 649.
(6) Fytas, G.; Dorfmüller, Th.; Lin, Y.-H.; Chu, B. *Macromolecules* **1981**, *14*, 1088.
(7) Wang, C. H.; Fytas, G.; Lilge, D.; Dorfmüller, Th. *Macromolecules* **1981**, *14*, 1363.
(8) Patterson, G. D.; Stevens, J. R.; Lindsey, C. P. *J. Macromol. Sci., Phys.* **1981**, *B18*, 641.
(9) Fytas, G.; Patkowski, A.; Meier, G.; Dorfmüller, Th. *Macromolecules* **1982**, *15*, 214.
(10) Williams, G.; Watts, D. C. In *NMR Basic Princ. Prog.* **1971**, *4*, 271.
(11) Miller, A. A. *Polymer* **1979**, *20*, 927.
(12) Sanchez, I. C. *J. Appl. Phys.* **1974**, *45*, 4204.
(13) Dux, H.; Dorfmüller, Th. *J. Chem. Phys.* **1979**, *40*, 219.
(14) Chu, B.; Fytas, G.; Zalczer, G. *Macromolecules* **1981**, *14*, 398.
(15) Gulari, Es.; Gulari, Er.; Tsunashima, Y.; Chu, B. *J. Chem. Phys.* **1979**, *70*, 3965.
(16) Miller, A. A. *Macromolecules* **1978**, *11*, 859.
(17) Helfand, E. *J. Chem. Phys.* **1971**, *54*, 4651.
(18) Lindsey, C. P.; Patterson, G. D. *J. Chem. Phys.* **1980**, *73*, 3349.

Light Scattering Study of a Series of Xanthan Fractions in Aqueous Solution

Gaio Paradossi and David A. Brant*

Department of Chemistry, University of California, Irvine, California 92717.
Received December 29, 1981

ABSTRACT: A series of fractions of xanthan polysaccharide (Kelco Keltrol) has been prepared by ultrasonic degradation and subsequent molecular weight fractionation on preparative-scale size exclusion chromatography columns packed with controlled pore glass (Electronucleonics CPG-10). The samples were converted to the sodium salt form and studied in 0.1 M aqueous NaCl solution. They were characterized by NMR, ORD, and UV absorption spectroscopy and are believed to be chemically equivalent to the undegraded starting material. Twelve xanthan samples covering a range of $\bar{M}_w$ from 0.8×10^5 to 19.5×10^5 were studied by Rayleigh light scattering. The radii of gyration and second virial coefficients were found to depend on molecular weight in the way expected for samples of molecularly dispersed, semiflexible macromolecules. For the samples of higher molecular weight the angular dependence of the scattering intensity exhibited asymptotic behavior at high angle and could be analyzed directly to give a linear mass density of about 2000 daltons/nm. Assuming that the samples of lower molecular weight behave as rigid rods, it was also possible to analyze the scattering curves for these samples in the limiting (low angle) region to yield the linear mass density. Although these data are more scattered due to uncertainties arising from the correction for molecular weight heterogeneity, they yield a linear mass density fully consistent with the value obtained from the asymptotic behavior of the high molecular weight samples. These results support the proposal by Holzwarth that xanthan exists in aqueous solution as double-stranded helical chains.

The bacterial polysaccharide xanthan is of interest not only for its commercial applications,[1,2] but also because it is known to undergo transitions in conformation which can be driven by changes in temperature, ionic strength, and the degree of ionization of the polymeric carboxyl groups.[3-9] Although the chemical constitution of the polymer now seems firmly established (cellulosic backbone with ionic three-sugar side chains on alternating backbone residues),[10,11] the polymer chain conformation remains a matter of some discussion [3-9,12-21] The present work has been undertaken in an attempt to deduce from Rayleigh light scattering some additional information about the stiffness of the xanthan chain in dilute solution and the linear mass density of the molecule.

The limiting (low angle) dependence of Rayleigh scattered light from an infinitely dilute solution of macromolecules, chemically homogeneous but heterogeneous with respect to molecular weight, is well-known to yield the mean-square z-average radius of gyration $\langle s^2 \rangle_z$ regardless of particle shape, provided certain basic conditions are met.[22] The same experiment yields the weight-average molecular weight $\bar{M}_w$ of the particles and, if the concentration dependence of the scattering at zero scattering angle is analyzed, a complicated average of the osmotic second virial coefficient A_2' may be obtained.[23] If the solvent comprises more than one component, then special experimental procedures are required in general to obtain the true molecular weight and virial coefficient of the macromolecular component.[24] Data of this sort are normally analyzed by using the equation

$$\frac{Kc_2}{\alpha i(\theta)} = \frac{1}{\bar{M}_w}\left[1 + \frac{\mu^2\langle s^2\rangle_z}{3}\right] + 2k^{-1}A_2'c_2 \qquad (1)$$

where K and α are standard optical parameters defined elsewhere,[25,26] c_2 is the polymer concentration in g/mL, $i(\theta)$ is the excess scattering at angle θ due to dissolved polymer, μ is the magnitude of the scattering vector defined by μ

0024-9297/82/2215-0874$01.25/0

$= 4\pi \sin(\theta/2)/(\lambda/n)$ with wavelength in vacuo λ and refractive index n, and k is an arbitrary constant chosen to facilitate convenient extrapolations of the data to vanishing c_2 and θ.[27]

For linear chains the quantity $\langle s^2\rangle_z^{1/2}$ obtained from scattering in the limiting angular domain may be shown[22,23,28] to correspond to the polymeric species having a molecular weight which lies in the range $\bar{M}_z$ to $(\bar{M}_z\bar{M}_{z+1})^{1/2}$ inclusive, depending on the form of the polymer chain. The lower limit refers to Gaussian random coils, the upper limit is for rigid, rodlike molecules, and wormlike chains, depending on their stiffness, fall somewhere between these limits.

Because xanthan is a stiff and extended macromolecule, it proved possible with some of the xanthan samples studied in this investigation to analyze the scattering behavior in the high-angle asymptotic domain. From these data one may obtain the linear mass density (i.e., mass per unit length M/L) for rods or wormlike chains of uniform cross section irrespective of molecular weight heterogeneity.[22,23,28] Equation 2,[28,29] valid for $\mu L \gg 1$ (but only

$$\lim_{c_2\to 0}\left(\frac{\mu\alpha i(\theta)}{\pi K c_2}\right) = \frac{M}{L} - \frac{2M}{\pi\mu L^2} \qquad (2)$$

when $\mu r \ll 1$, where r is the radius of the chain cross section), shows that a plot of $\mu\alpha i(\theta)/\pi K c_2$ at vanishng c_2 against μL (or $\mu\langle s^2\rangle_z^{1/2}$) will reach an asymptote equal to M/L for large μL.

Experimental Section

Preparation of Degraded Polymer Samples. All samples were prepared from commercial food grade xanthan (Keltrol lot no. KTL 23070-76, Kelco). The polymer was dissolved in distilled water to a concentration of ca. 5 g/L by vigorous stirring overnight with a "Lightnin" laboratory mixer and centrifuged at 9000 rpm for 2 h in a Sorvall RC2-B centrifuge using a GS-3 rotor. The supernatant was decanted for subsequent sonication.

The centrifuged polymer solution was sonicated in 500-mL batches using a Branson Model 185 sonicator (150 W, 20 kHz) at maximum allowed power with either a macroprobe (1-cm diameter) or microprobe (2-mm diameter). Acetone (5 mL) was added to the solution being sonicated as a free radical scavenger, and the solution was cooled with ice and swept with N_2 gas during the sonication. Some batches were sonicated for 2 h (microprobe) and pooled (XS2H); another group was sonicated for 10–14 h (macroprobe) and pooled (XS12H). The progress of the sonications was monitored by size exclusion chromatography (SEC) as described below.

Solutions XS2H and XS12H were centrifuged for 1 h as described above, filtered through 0.45-μm Millipore filters, dialyzed against 0.01 M EDTA, and finally dialyzed exhaustively against purified water (Millipore Milli-Q) until the presence of titanium ions from the sonicator probe could not be detected in the dialysate by a sensitive specific assay.[30] Cations in the dialyzed solutions were then exchanged with Mallinckrodt IR 120 resin in the Na^+ form to obtain the sodium salt of the polymer. Finally solutions XS2H and XS12H were concentrated on a rotatary evaporator to a concentration of ca. 5 g/L.

Size Exclusion Chromatography. Size exclusion chromatography was used in the analytical and preparative modes. All columns were packed with controlled pore glass (CPG-10, Electronucleonics). Analytical SEC was performed with a set of three stainless steel columns (30 cm × 0.46 cm i.d.) in series, packed, respectively, with a water slurry of CPG-10 in pore sizes 224, 729, and 2734 Å; a 10-cm guard column packed with pore size 172 Å was also used. Eluant (freshly degassed 0.05 M aqueous Na_2SO_4) was delivered at 1 mL/min, and a differential refractometer was used as detector. The progress of the sonication was readily monitored with this arrangement. The position of the maximum of the polymer peak, normalized to the span of elution volume between the exclusion and permeation volumes of the column set, was a linear function of log $(t + 1)$, where t is the time of sonication in minutes, in the range 30–1000 min.[31] This circumstance facilitated preparation of samples with predetermined extents of degradation. The columns were also useful for qualitative assessment of the molecular weight distributions (MWD) of fractions made using preparative SEC; we were, however, unable to use these columns successfully for quantitative determination of the MWD of our xanthan samples.

Solutions XS2H and XS12H were chromatographed on a set of two preparative SEC columns (95 cm × 2.6 cm i.d., LKB Instruments) in series, packed, respectively, with CPG-10 in pore sizes 324 and 1038 Å. The columns were loaded with 15–50 mL of solution, depending on the viscosity, with a syringe pump (Model 341, Sage Instruments) and eluted with freshly degassed 0.05 M aqueous Na_2SO_4 at ca. 200 mL/h. Use of an LKB Ultrorac II fraction collector with a Varioperpex II pump and a Uvicord SUV detector (λ = 206 nm) facilitated pooling of fractions from the successive chromatographic runs required to accumulate polymer samples of sufficient size for experimental characterization. Four pooled xanthan fractions (XF1–XF4) were prepared from solution XS2H and six (XF1C–XF6C) from solution XS12H. Each fraction was dialyzed exhaustively against Milli-Q water until SO_4^{2-} could no longer be detected in the dialysate with a saturated $BaCl_2$ solution and then concentrated on a rotary evaporator to concentrations ranging from 2 to 8 g/L. These stock solutions were stored at 2 °C; polymer samples recovered as lyophylized solids did not yield consistent light scattering results when redissolved. In addition to these 10 fractions, the unfractionated sample XS2H and the unsonicated starting material (XU1), purified following Holzwarth,[3] were studied. The concentrations of all stock solutions were determined by dry weight analysis.[26]

^{1}H NMR Spectroscopy. Aliquots (10 mL) of the above stock solutions were lyophylized and the dry polymer samples were weighed. Each sample was then dissolved in D_2O and lyophylized 3 times to replace the exchangeable protons with deuterium, and the fully exchanged sample was dissolved in a weighed amount of D_2O to yield a solution of ca. 8 g/L. A solution of p-dichlorobenzene (0.104 M) and Me_4Si (1%) in CCl_4 was placed in a concentric capillary tube to provide, respectively, a standard for computing proton concentrations from peak areas and a chemical shift reference. Spectra were recorded at 85 °C with a Bruker WM-250 at 250 MHz in the quadrature FT mode, accumulating 100–200 scans at a repetition rate of 10 s and with sweep width 2500 Hz and a frequency offset 4800 Hz. The pyruvyl and acetyl contents of the samples were then calculated from their respective measured peak areas A_p and that of the p-dichlorobenzene proton reference A_r using the equation[32] $c_p = (4A_p/3A_r)(R_r^2/(R_p^2 - R_r^2))c_r$, where c_p is the molarity of pyruvyl or acetyl, c_r is the molarity of p-dichlorobenzene, R_r is the radius of the reference capillary (0.5 mm), and R_p is the radius of the sample tube (2.5 mm).

ORD and UV Measurements. Measurements were made directly on the salt-free stock solutions. Jacketed 5-cm cells with quartz windows were used to measure the ORD in the range 256–550 nm at 25 °C with a Perkin-Elmer 241 MC spectropolarimeter. Absorbance measurements were made at room temperature with 1-cm quartz cells in the range 200–320 nm using a Zeiss PM6 spectrophotometer.

Measurements of Specific Refractive Index Increment. The specific refractive index increment $(\partial n/\partial c_2)_{\mu,T}$ required in the optical constant K of eq 1 for light scattering in multicomponent systems[24–26] was measured at 27 °C with a Brice-Phoenix differential refractometer on solutions prepared as follows: Solid NaCl was added to ca. 25 mL of a salt-free xanthan stock solution to yield a solution 0.100 M in NaCl. The resulting three-component stock solution was placed in a stirred, constant-volume dialysis cell and dialyzed using preconditioned Schleicher and Schuell Type RC52 membranes against a 20-fold excess of stirred aqueous 0.100 M NaCl for 36 h. This dialyzed stock solution was used directly, with dialysate as reference, to determine $(\partial n/\partial c_2)_{\mu,T}$. It was subsequently diluted volumetrically with dialysate to yield solutions employed for additional differential refractometry as well as for the light scattering and osmotic pressure measurements. The quantity $(\partial n/\partial c_2)_{c,T}$, measured at constant molarity rather than at constant chemical potential of membrane-diffusible components, was also determined on the undialyzed three-component stock solution of each xanthan sample.

Table I
Characteristics of the Xanthan Samples

fraction	$\bar{M}_n \times 10^{-5}$	$\bar{M}_w \times 10^{-5}$	$A_2' \times 10^4$, (mL mol)/g^2	DS_{pyr}	DS_{ace}	$[\alpha]^{25}_{302}$, (deg mL)/(g dL)	$\langle s^2 \rangle_z^{1/2}$, nm
XU1		19.5	4.7	0.6	0.9	−46	137
XF1		15 ± 1.7	5.35 ± 0.01	0.6	1.2	−56	150 ± 5
XF2		8.4 ± 0.3	6.13 ± 0.30	0.6	0.9	−57	113 ± 6
XF3		6.8 ± 1.2	6.10 ± 0.04	0.5	0.9	−80	101 ± 6
XS2H	1.22	6.3	6.1				102
XF4		5.6 ± 0.3	6.4 ± 0.8	0.2	0.6	−75	88 ± 4
XF1C		3.3 ± 0.02	7.3 ± 1.1	0.4	0.4	−27	57 ± 0.3
XF2C		3.6 ± 0.1	5.5 ± 0.5	0.2	0.4	−45	62 ± 1
XF3C	2.3	2.4	4.2	0.6	1.0	−70	55
XF4C	1.6 ± 0.1	1.7 ± 0.06	6.8 ± 0.2	0.6	1.1		36 ± 3
XF5C	0.95	1.4 ± 0.01	7.0 ± 0.5	0.6	1.0		31
XF6C		0.8	13				23

Light Scattering Measurements. Light scattering measurements were made with a SOFICA Model 42000 instrument using unpolarized incident light of wavelength 436 nm. The scattering cells were of the floatable type already described.[26] Dialyzed polymer solutions and dialysate prepared as described above were filtered through 0.45- or 3-μm Millipore filters into the scattering cells and then centrifuged for 2 h at 17 000 rpm in a Spinco SW 25.1 rotor. The photometer was calibrated with dedusted benzene and the instrument alignment was verified by confirming that the angular dependence of the scattering from several pure liquids and dilute aqueous salt solutions yielded the expected depolarization ratio.[26] Scattering intensities were measured at 27 °C in the angular range $30 \leq \theta \leq 150°$ on five xanthan solutions of different concentrations and on the dialysate. Data for all samples were processed according to eq 1 and 2. In using eq 1 the concentration dependence at $\theta = 0$ was fit with a linear least-squares curve from which A_2' was obtained. The angular dependence at $c_2 = 0$ was always fit with a least-squares polynomial of second degree, and $\langle s^2 \rangle_z$ was obtained from the limiting slope of the least-squares curve. Only for the more highly degraded fractions (XF1C–XF6C) did the function $\mu^2\langle s^2 \rangle_z$ extend into the range below 0.5, where the limiting behavior implied by eq 1 can safely be anticipated.[28] On the other hand, only the six samples of highest molecular weight (XF1–XF4, XS2H, and XU1) displayed the asymptotic behavior described by eq 2.

Osmotic Pressure Measurements. Osmotic pressure measurements were made at 34 °C on the same solutions used for light scattering with a Mechrolab Model 502 membrane osmometer using Schleicher and Schuell Type AC62 membranes. Experimental procedures and data processing have been described previously.[26]

Results and Discussion

Most of the pertinent experimental results are summarized in Table I, where it can be seen in columns 2 and 3 that a 24-fold range of molecular weights ($\bar{M}_w$) has been investigated. Table entries without any indication of experimental uncertainty are based on a single observation. Entries showing uncertainties represent averages over two or more measurements. The fractions were eluted from the preparative SEC columns in the order expected; i.e., fractions XF1 and XF1C were eluted first and fractions XF4 and XF6C were eluted last in the respective fractionations of solutions XS2H and XS12H. Only in the case of fractions XF1C and XF2C was there an inversion of the expected order of elution. Unfractionated sample XS2H is seen from its values of $\bar{M}_n$ and $\bar{M}_w$ to be broadly distributed, and its $\bar{M}_w$ falls in the lower part of the range of $\bar{M}_w$ values characterizing the four fractions derived from it. Unfractionated sample XU1 has $\bar{M}_w \simeq 2 \times 10^6$, which is higher than that of any fraction derived from the sonicated samples.

Refractive Increment. The mean value of $(\partial n/\partial c_2)_{\mu,T}$ determined in these studies was 0.144 ± 0.002 mL/g, in reasonable agreement with earlier results on xanthan in aqueous medium[5,17] and as anticipated from experience, with many other polysaccharides in aqueous solution; there was no detectable dependence on xanthan molecular weight in the range investigated. In some measurements of $(\partial n/\partial c_2)_{\mu,T}$ an anomalously small value was obtained. This problem is believed to arise from absorption of xanthan on the cellulosic material of the dialysis membrane.[4] Light scattering from the dialysate phase was always normal in these cases, indicating that the small refractive increment did not result from leakage of polymer from the dialysis cell. Because the largest measured values of $(\partial n/\partial c_2)_{\mu,T}$, i.e., the value quoted above, were always indentical with $(\partial n/\partial c_2)_{c,T}$ measured on the undialyzed xanthan stock solutions, we believe there is no sensible difference between $(\partial n/\partial c_2)_{\mu,T}$ and $(\partial n/\partial c_2)_{c,T}$ in this system. We have consequently processed all light scattering data using the mean value of $(\partial n/\partial c_2)_{\mu,T}$ reported above. In those experiments in which an anomalously small value of $(\partial n/\partial c_2)_{\mu,T}$ was observed, the ratio of the observed value to 0.144 mL/g was used to determine the concentration of dissolved xanthan in the dialyzed stock solution.

Pyruvyl and Acetyl Substitution. Pyruvyl and acetyl substitution was measured by ^{1}H NMR on 10 of the 12 samples. Seven of these samples display $DS_{pyr} \simeq 0.6$ and $DS_{ace} \simeq 1.0$ (see columns 5 and 6 of Table I). Fractions XF4, XF1C, and XF2C show smaller degrees of substitution for both moieties. The correspondingly lower linear charge density on these samples may be related to the anomalous SEC elution of XF1C and XF2C. The latter two fractions display relatively smaller specific rotations (see column 7 of Table I), but in other respects (see below) all three fractions show a behavior completely consistent with the other nine samples.

It is interesting to remark that the ^{1}H NMR peaks corresponding to the pyruvyl and acetyl protons are observed at room temperature for the lower molecular weight samples, whereas higher temperatures are required for samples of higher molecular weight.[4] With fraction XF5C, for example, the two signals appear as sharp peaks at 25 °C which, nevertheless, increase in area to a limiting value as the temperature is increased. This observation is consistent with the report of Milas and Rinaudo[7] that the conformational transition temperature observable in xanthan with several techniques diminishes with decreasing polymer molecular weight when pH and salt concentration are held constant.

Optical Properties. The specific rotations at 25 °C and $\lambda = 302$ nm of 8 of the 12 xanthan samples are reported in column 7 of the table and serve to indicate the relative positions of the ORD curves measured on the salt-free xanthan stock solutions. The present samples exhibit specific rotations comparable in magnitude to those re-

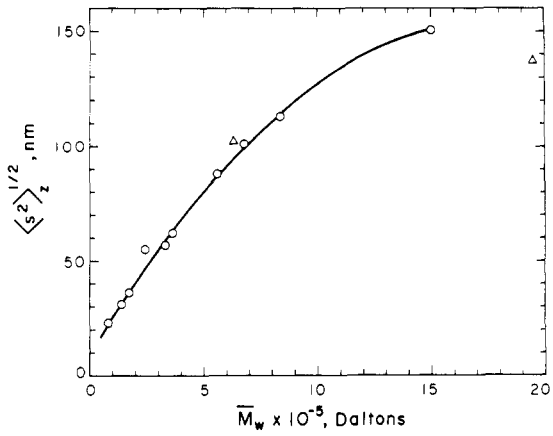

Figure 1. Plot of the root-mean-square radius of gyration $\langle s^2 \rangle_z^{1/2}$ vs. the weight-average molecular weight $\bar{M}_w$ for xanthan fractions (open circles) and unfractionated samples (open triangles).

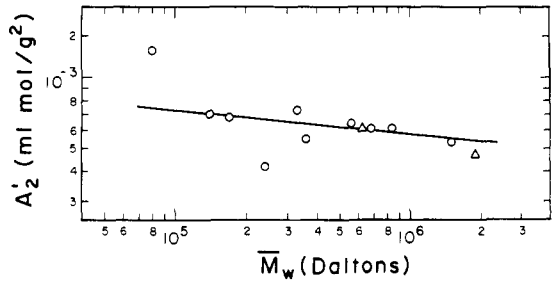

Figure 2. Logarithmic plot of the osmotic second virial coefficient A_2' from light scattering vs. the weight-average molecular weight $\bar{M}_w$ for xanthan fractions (open circles) and unfractionated samples (open triangles).

ported by other workers.[3,4] We find no consistent correlation between ORD and the molecular weights or degrees of pyruvyl and/or acetyl content of the samples. Such a correlation, if it exists, may be masked by the known sensitvity of xanthan optical activity to the thermal history of the samples in salt-free solutions.[3]

The UV absorption spectra of the xanthan samples served as a useful check on their purity. The unsonicated (XU1) and unfractionated (XS2H) samples displayed characteristic shoulders in their spectra at 280 nm, which were completely absent in the spectra of the fractionated samples. The sonicated samples, including XS2H, did not exhibit the troublesome low-wavelength scattering that was evident from the unsonicated sample in both the ORD and UV absorption experiments.

Light Scattering. Root-mean-square radii of gyration $\langle s^2 \rangle_z^{1/2}$ from eq 1 are plotted vs. $\bar{M}_w$ in Figure 1. Nine of the twelve points fall on a single smooth curve drawn through the data; only the point for undegraded sample XU1 deviates significantly from this curve, and a second deviant point corresponds to the unfractionated sample XS2H. The measured virial coefficients A_2' are plotted against $\bar{M}_w$ in logarithmic representation in Figure 2; only two of the points depart substantially from a linear correlation drawn through the data. In particular, the $\langle s^2 \rangle_z^{1/2}$ and A_2' values for fractions XF4, XF1C, and XF2C, which show anomalously low degrees of pyruvyl and acetyl substitution, conform well to the general pattern established by the other samples, and we find no reason to disregard these three fractions in the present analysis. We assume throughout, on the basis of results on other highly asymmetric polymer chains,[33–35] that any correction of the light scattering data for optical anisotropy[22,28] will be negligible.

The plot of $\langle s^2 \rangle_z^{1/2}$ vs. $\bar{M}_w$ shows the curvature expected of a semiflexible polymer chain.[15,16] The measured chain

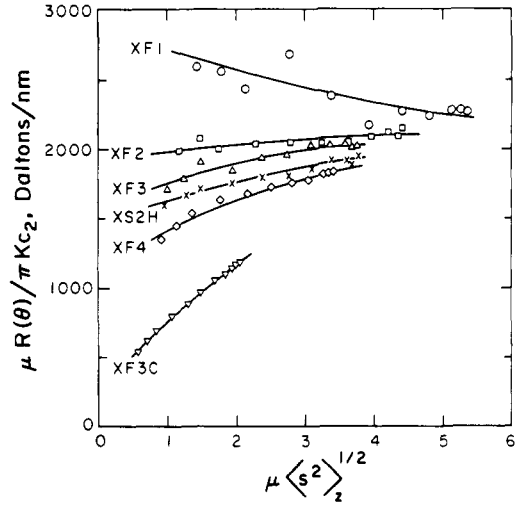

Figure 3. Plots of $\lim_{c_2 \to 0} (\mu R(\theta)/\pi K c_2)$ vs. $\mu \langle s^2 \rangle_z^{1/2}$ according to eq 2 for several xanthan samples.

extension is large and achieves values, relative to the molecular weight, greater than observed for the double-stranded nucleic acids and other stiff cellulose derivatives (see below). The small negative slope (–0.10) of the logarithmic plot of A_2' vs. $\bar{M}_w$ is also consistent with the chain stiffness suggested by the measured radii of gyration.[36,37] Radii of gyration reported for the six samples of higher molecular weight may be smaller than the true values, because the accessible angular range of the light scattering photometer did not allow the measurements to extend into the limiting domain of $\mu^2 \langle s^2 \rangle_z$ required for confidence in application of eq 1. In an effort to combat this difficulty, $\langle s^2 \rangle_z$ was always obtained from the initial slope of a quadratic fit to the angular dependence extrapolated to zero concentration. For the six samples of lower molecular weight, which are evidently nearly rodlike, it is more appropriate to plot $\langle s^2 \rangle_z^{1/2}$ against $(\bar{M}_z \bar{M}_{z+1})^{1/2}$. Replotting in this way would shift the lower part of the curve in Figure 1 to the right, in the direction required to correct the apparent failure of the curve to pass through the origin (see Figure 4, discussed below). The $\langle s^2 \rangle_z^{1/2}$ values for the six higher molecular weight samples should also be plotted against a molecular weight average somewhat higher than $\bar{M}_z$. Corrections to the curve in Figure 1 for molecular weight heterogeneity and possible inaccuracies in the larger values of $\langle s^2 \rangle_z^{1/2}$ seem unlikely to remove the curvature in Figure 1 attributed to chain flexibility.

When the scattering data are analyzed according to eq 2, it is found that only for the six samples of larger $\bar{M}_w$ is the asymptotic behavior realized. Data plotted according to eq 2 in Figure 3 for samples XF1–XF4, XS2H, and XF3C illustrate this point. The lower molecular weight sample XF3C clearly does not attain the asymptote, whereas sample XF1 approaches the asymptote from above, as expected for long, stiff chains exhibiting some flexibility.[28] Because the data on the unsonicated, unfractionated sample XU1 do not agree well with the trend dictated by the sonicated and fractionated samples in Figure 1, XU1 is omitted from consideration in Figure 3. The upper five curves in Figure 3 appear to converge to an asymptote corresponding to a linear mass density of about 2000 daltons/nm. It is significant that, in accordance with the expected independence of this analysis of molecular weight heterogeneity, the unfractionated sample XS2H conforms exactly to the pattern established by the fractionated samples.

If the six fractions of lower molecular weight can be assumed to be rodlike, then the length of the rod may be

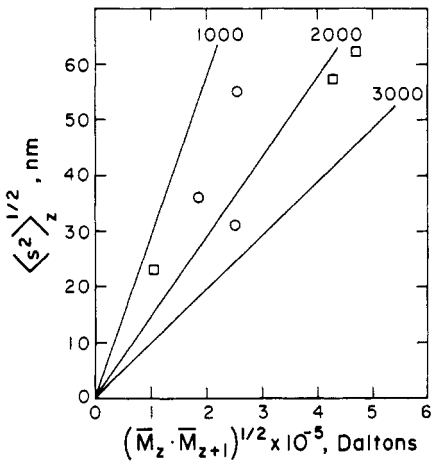

Figure 4. Plot of the root-mean-square radius of gyration $\langle s^2 \rangle_z^{1/2}$ vs. the geometric mean of the z and $z + 1$ averages of the molecular weight $(\bar{M}_z\bar{M}_{z+1})^{1/2}$ for xanthan fractions XF1C–XF6C. Open circles denote data for which the molecular weight heterogeneity index $\bar{M}_w/\bar{M}_n$ was measured; open squares refer to data for which $\bar{M}_w/\bar{M}_n$ was estimated. Solid lines describe the behavior expected for rodlike molecules with linear mass densities of 1000, 2000, and 3000 daltons/nm, respectively.

computed[22,37] from $L = (12\langle s^2 \rangle_z)^{1/2}$, and this length combined with $(\bar{M}_z\bar{M}_{z+1})^{1/2}$ to obtain the linear mass density of the low molecular weight fractions from their scattering behavior in the limiting angular domain. In pursuit of this approach we have plotted $\langle s^2 \rangle_z^{1/2}$ vs. $(\bar{M}_z\bar{M}_{z+1})^{1/2}$ for these fractions in Figure 4, where the straight lines passing through the origin are drawn to correspond to the behavior expected for rods with linear mass densities of 1000, 2000, and 3000 daltons/nm. Values of $\bar{M}_z$ and $\bar{M}_{z+1}$ have been estimated for fractions XF3C, XF4C, and XF5C using the measured values of $\bar{M}_n$ and $\bar{M}_w$ by assuming a log-normal molecular weight distribution for which $\bar{M}_w/\bar{M}_n = \bar{M}_z/\bar{M}_w = \bar{M}_{z+1}/\bar{M}_z$.[23] For fractions XF1C, XF2C, and XF6C $\bar{M}_z$ and $\bar{M}_{z+1}$ were estimated from their measured $\bar{M}_w$ values by assuming that the *mean* value of $\bar{M}_w/\bar{M}_n$ observed for fractions XF3C–XF5C was applicable. Although the data in Figure 4 are scattered, primarily as a consequence of the heterogeneity correction, they appear to be consistent with the linear mass density deduced from the asymptotic behavior of the high molecular weight samples. Assumption of a Zimm–Schulz molecular weight distribution[23] instead of the log-normal distribution leads to slightly larger values of $(\bar{M}_z\bar{M}_{z+1})^{1/2}$ and, hence, does not alter this conclusion.

In considering the results in Figure 4 it is worth noting that the point which deviates most from the line for M/L = 2000 daltons/nm corresponds to fraction XF3C, for which it appears from Figure 1 that the measured ratio of mass to length is anomalously low. On the other hand, if any of the fractions dealt with in Figure 4 have large enough chain lengths to be somewhat flexible rather than perfectly rodlike, the present analysis will overestimate the true linear mass density of the chain. It should also be observed that although the lower molecular weight samples gave some evidence in their ^{1}H NMR spectra of being in the "disordered" state at room temperature, the ^{1}H NMR experiments were done in the absence of salt whereas the ionic strength in the light scattering experiments was high enough to have moved the transition temperatures to well above room temperature.[7]

Analysis of X-ray diffraction patterns from xanthan fibers[12,13] suggests that the chains in the crystalline regions of these fibers adopt a fivefold helical conformation characterizated by a projection on the helical axis of 0.94 nm per repeating unit. Since the mass per repeating unit of a xanthan sample with DS_{pyr} = 0.6 and DS_{ace} = 1.0 is 966 daltons, the linear mass density of such rigid, helical chains would be close to 1000 daltons/nm. Considerations of the fiber density and the possible packing arrangements of the crystalline xanthan chains indicate, however, that the crystalline chains probably occur as double-stranded helices with twice the linear mass density of the single chains.[13] Holzwarth has presented evidence, based on an hydrodynamic analysis of ultrasonically degraded xanthan samples,[15] that the polymer in aqueous solution also has a linear mass density of about 2000 daltons/nm. Thus, it is suggested that xanthan in dilute aqueous solution exists as paired chains which preserve to a large degree the ordered crystalline conformation.[14] All evidence, including the present light scattering results, demonstrates that the dissolved polymer is very stiff. Given this circumstance and the present strong indication of a linear mass density of 2000 daltons/nm, the existence of paired xanthan strands in solution appears quite probable. In order to achieve the observed linear mass density, a single-stranded, inflexible conformation of xanthan would have to display a repeat-unit projection on the pseudohelical axis so small as to be energetically quite unrealistic for chains possessing a cellulosic backbone.[38,39] The present experiments, however, obviously cannot distinguish between double-stranded xanthan species formed by pairing of two separate chains or by folding of one single chain.

It might be argued that the linear mass density observed in the present experiments reflects not a specific pairing of chains but rather the *mean* behavior of chains which have a propensity for side-by-side aggregation. There is no evidence in the light scattering results for this interpretation. In such a situation the asymptotic behavior predicted by eq 2 is no longer expected, but rather the contribution to the scattering function from the cross section of the larger aggregates causes the plateau at large values of $\mu\langle s^2 \rangle_z^{1/2}$ to decay.[28,29] This behavior is not observed in the present results. Futhermore, the extent of nonspecific aggregation might be expected to show a dependence on molecular weight, but we obtain effectively the same mass per unit length from observations at both ends of the 24-fold molecular weight range investigated. Finally, reversible, nonspecific aggregation would be expected to manifest itself in the measured virial coefficients, which are, in fact, as anticipated for a series of molecularly dispersed fractions of differing mean molecular weight.

We conclude by observing that the chain extension of xanthan measured in these studies is very much greater than that of other highly substituted cellulosics, which certainly exist in solution predominantly as molecularly dispersed single chains. A comparison of xanthan with aqueous (carboxymethyl)cellulose, especially with respect to the polyelectrolyte behavior, has already been provided;[18] here we focus specifically on cellulose tricarbanilate (CTC)[40] and cellulose acetate (CA) with a degree of substitution 2.45[41] for which the dimensionless characteristic ratio $\langle s^2 \rangle_0/xL^2$ has the value 7.5 and 6.0, respectively, in the asymptotic domain of high chain length. Here $\langle s^2 \rangle_0$ is the unperturbed mean-square radius of gyration of a chain containing x glucose residues each of length L = 5.45 Å. For the highest molecular weight xanthan fractions XF1, XF2, and XF3 the quantity $\langle s^2 \rangle_z/\bar{x}_wL^2$ takes the mean values 25 and 50, assuming single- and double-stranded behavior, respectively. This striking comparison of xanthan with the two other cellulosics clearly would not be substantially altered by appropriate correction of the weight-average number of glucose residues $\bar{x}_w$ for chain

length heterogeneity or by the small[42] correction of $\langle s^2 \rangle_z$ to the unperturbed state.

The CTC and CA chains possess much more densely substituted backbones than xanthan. In particular, CTC has three large phenylcarbamate substituent groups per glucose residue; its large characteristic ratio reflects the considerable conformational constraint thereby imposed.[43] It is difficult to understand the much greater conformational constraint which evidently exists in xanthan unless the freedom of the chain backbone is limited by its involvement in a specific multistranded aggregate or, as has often been suggested,[5,9] by a strong interaction with the three-sugar side chains, which must in this case be folded into some very regular pattern of juxtaposition. The measured linear mass density of about 2000 daltons/nm clearly favors the former explanation. It is interesting to note that on the basis of comparisons of $\langle s^2 \rangle_z / \bar{M}_w$ values, xanthan is in fact more extended than double-stranded DNA and has an extension comparable to the 1,3-linked β-D-glucan schizophyllan, which has been clearly demonstrated to exist as a triple-stranded helix in aqueous solution.[34] For samples with molecular masses in the range (1–5) × 10^6 daltons, $\langle s^2 \rangle_z / \bar{M}_w = 1.5 \times 10^{-2}$, 0.5×10^{-2}, and 1.5×10^{-2} nm²/dalton, respectively, for xanthan, DNA,[42] and schizophyllan.[34] On this basis DNA is in fact rather more like CTC, for which $\langle s^2 \rangle_z / \bar{M}_w = 0.4 \times 10^{-2}$/dalton.

Acknowledgment. This paper was supported by NIH Grant No. 5 R01 AI 15096 and NSF Grant No. PCM79-23041. Initial aspects of the work were undertaken by Dr. Donald S. Clark, whose contributions, particularly with regard to the preparative and analytical SEC procedures, we acknowledge with thanks.

References and Notes

(1) Sandford, P. A.; Laskin, A. I., Eds. "Extracellular Microbial Polysaccharides"; American Chemical Society: Washington, D.C., 1977; ACS Symp. Ser., No. 45.
(2) Brant, D. A., Ed. "Solution Properties of Polysaccharides"; American Chemical Society: Washington, D.C., 1981; ACS Symp. Ser., No. 150.
(3) Holzwarth, G. *Biochemistry* **1976**, *15*, 4333.
(4) Morris, E. R.; Rees, D. A.; Young, G.; Walkinshaw, M. D.; Darke, A. *J. Mol. Biol.* **1977**, *110*, 1.
(5) Milas, M.; Rinaudo, M. *Carbohydr. Res.* **1979**, *76*, 189.
(6) Norton, I. T.; Goodall, D. M.; Morris, E. R.; Rees, D. A. *J. Chem. Soc., Chem. Commun.* **1980**, 545.
(7) Milas, M.; Rinaudo, M. In ref 2, Chapter 3.
(8) Southwick, J. G.; Jamieson, A. M.; Blackwell, J. In ref 2, Chapter 1.
(9) Rees, D. A. *Pure Appl. Chem.* **1981**, *53*, 1.
(10) Jansson, P. E.; Kenne, L.; Lindberg, B. *Carbohydr. Res.* **1975**, *45*, 275.
(11) Melton, L. D.; Mindt, L.; Rees, D. A.; Sanderson, G. R. *Carbohydr. Res.* **1976**, *46*, 245.
(12) Moorhouse, R.; Walkinshaw, M. D.; Arnott, S. In ref 1, Chapter 7.
(13) Okuyama, K.; Arnott, S.; Moorhouse, R.; Walkinshaw, M. D.; Atkins, E. D. T.; Wolf-Ullish, Ch. In "Fiber Diffraction Methods"; French, A. D., Gardner, K. H., Eds.; American Chemical Society: Washington, D.C., 1980, Chapter 26; ACS Symp. Ser., No. 141.
(14) Holzwarth, G.; Prestridge, E. B. *Science* **1977**, *197*, 757.
(15) Holzwarth, G. *Carbohydr. Res.* **1978**, *66*, 173.
(16) Holzwarth, G. In ref 2, Chapter 2.
(17) Dintzis, F. R.; Babcock, G. E.; Tobin R. *Carbohydr. Res.* **1970**, *13*, 257.
(18) Rinaudo, M.; Milas, M. *Biopolymers* **1978**, *17*, 2663.
(19) Maret, G.; Milas, M.; Rinaudo, M. *Polym. Bull.* **1981**, *4*, 291.
(20) Southwick, J. G.; McDonnell, M. E.; Jamieson, A. M.; Blackwell, J. *Macromolecules* **1979**, *12*, 305.
(21) Southwick, J. G.; Lee, H.; Jamieson, A. M.; Blackwell, J. *Carbohydr. Res.* **1980**, *84*, 287.
(22) Geiduschek, E. P.; Holtzer, A. *Adv. Biol. Med. Phys.* **1958**, *6*, 431.
(23) Elias, H.-G.; Bareiss, R.; Watterson, J. G. *Adv. Polym. Sci.* **1973**, *11*, 111.
(24) Casassa, E. F.; Eisenberg, H. *Adv. Protein Chem.* **1964**, *19*, 287.
(25) Jordan, R. C.; Brant, D. A. *Macromolecules* **1980**, *13*, 491.
(26) Goebel, K. D.; Brant, D. A. *Macromolecules* **1970**, *3*, 634.
(27) Zimm, B. H. *J. Chem. Phys.* **1948**, *16*, 1099.
(28) Eisenberg, H. In "Procedures in Nucleic Acid Research"; Cantoni, G. L., Davies, D. R., Eds.; Harper and Row: New York, 1971; Vol. 2, p 137.
(29) Mueller, M.; Burchard, W. *Biochim. Biophys. Acta* **1978**, *537*, 208.
(30) Kolthoff, I. M.; Elving, P. J., Eds. "Treatise on Analytical Chemistry"; Interscience: New York, 1961; Part II, Vol. 5.
(31) Basedow, A. W.; Ebert, K. *Adv. Polym. Sci.* **1977**, *22*, 83.
(32) Shefler, N. K. M.S. Thesis, University of California, Irvine, 1979.
(33) Godfrey, J. E.; Eisenberg, H. *Biophys. Chem.* **1976**, *5*, 301.
(34) Kashiwagi, Y.; Norisuye, T.; Fujita, H. *Macromolecules* **1981**, *14*, 1220.
(35) Noda, I.; Imai, T.; Kitano, T.; Nagasawa, M. *Macromolecules* **1981**, *14*, 1303.
(36) Yamakawa, H. "Modern Theory of Polymer Solutions"; Harper and Row: New York, 1971; Chapter 4.
(37) Tanford, C. "Physical Chemistry of Macromolecules"; Wiley: New York, 1961; Chapter 4.
(38) Rees, D. A.; Skerrett, R. J. *Carbohydr. Res.* **1968**, *7*, 334.
(39) Sathyanarayana, B. K.; Rao, V. S. R. *Biopolymers* **1971**, *10*, 1605.
(40) Burchard, W. *Br. Polym. J.* **1971**, *3*, 214.
(41) Tanner, D. W.; Berry, G. C. *J. Polym. Sci., Polym. Phys. Ed.* **1974**, *12*, 941.
(42) Borochov, N. Eisenberg, H.; Kam, Z. *Biopolymers* **1981**, *20*, 231.
(43) Hsu, B.; McWherter, C. A.; Brant, D. A.; Burchard, W. *Macromolecules*, in press.